

AIRMED: Efficient Self-Healing Network of Low-End Devices

Sourav Das*
University of Illinois at
Urbana-Champaign
souravd2@illinois.edu

Samuel Wadaj
Department of Computer Science and
Engineering., Indian Institute of
Technology Delhi
samuel.wed@cse.iitd.ac.in

Kolin Paul
Department of Computer Science and
Engineering., Indian Institute of
Technology Delhi
kolin@cse.iitd.ac.in

Umesh Bellur
Department of Computer Science and
Engineering, Indian Institute of
Technology Bombay
umesh@cse.iitb.ac.in

Vinay Joseph Ribeiro
Department of Computer Science and
Engineering, Indian Institute of
Technology Bombay
vinayr@iitb.ac.in

ABSTRACT

The proliferation of application specific cyber-physical systems coupled with the emergence of a variety of attacks on such systems (malware such as Mirai and Hajime) underlines the need to secure such networks. Most existing security efforts have focused on only detection of the presence of malware. However given the ability of most attacks to spread through the network once they infect a few devices, it is important to contain the spread of a virus and at the same time systematically cleanse the impacted nodes using the communication capabilities of the network. Toward this end, we present AIRMED - a method and system to not just detect corruption of the application software on a IoT node, but to self correct itself using its neighbors. AIRMED's decentralized mechanisms prevent the spread of self-propagating malware and can also be used as a technique for updating application code on such IoT devices. Among the novelties of AIRMED are a novel bloom-filter technique along with hardware support to identify position of the malware program from the benign application code, an adaptive self-check for computational efficiency, and a uniform random-backoff and stream signatures for secure and bandwidth efficient code exchange to correct corrupted devices. We assess the performance of AIRMED, using the embedded systems security architecture of TrustLite in the OMNeT++ simulator. The results show that AIRMED scales up to thousands of devices, ensures guaranteed update of the entire network, and can recover 95% of the nodes in 10 minutes in both internal and external propagation models. Moreover, we evaluate memory and communication costs and show that AIRMED is efficient and incurs very low overhead.

KEYWORDS

Device Correction; Internet-of-Things; Low End Devices; Malware Containment.

1 INTRODUCTION

Application-specific low-end devices have become ubiquitous in safety-critical systems such as hazard control, airplanes, nuclear reactors, etc. A recent Gartner report estimates that there will be more than 20 billion Internet-of-Things (IoT) devices by the end of

the year 2020 [2].¹ As the use of such devices becomes imperative in mission critical systems, their security is of immense concern [30]. Attacks on a nuclear power plant using Stuxnet [39], large scale Distributed-Denial-of-Service (DDoS) attacks using IoT Botnets such as Mirai and Hajime [7, 29], potential disruption of power-grids using high wattage devices [37], and malware which can rapidly spread citywide using deployed Phillips hue bulbs, illustrate the importance of ensuring that such networks are secure and/or can recover quickly and cheaply from attacks [33].

Existing security research on low-end devices only focuses on detecting the presence of malware using Remote Attestation (RA) [5, 8, 36] and Machine Learning (ML) [10, 20]. RA allows a trusted verifier to detect a compromised device or network of connected devices. Similarly, the core idea behind the ML-based detection of an attack is to train an ML model with historical network traces and use inferences to detect network intrusion in real-time.

Although these approaches are useful, their scope is limited. This is because, corrupt devices can not only malfunction, they can even spread the malware to other nodes. Furthermore, as we illustrate (ref. §5) an intelligent adversary can fatally prevent a significant fraction of honest nodes from correcting themselves via updates. Existing approaches fail to restrict a self-propagating malware from compromising the entire network [7, 11, 18, 29, 33]. Also, they do not tackle how to recover a compromised device in the presence of a root privileged adversary. A naive scheme of deploying a vulnerability patch over the network to update the corrupt device would not work because an adversary with access to the incoming network messages can simply drop the update messages. Finally, such efforts also make strong assumptions such as the trusted party can communicate with the network at all times; corrupted devices voluntarily communicate with a trusted party, and so on that rarely hold in real cyber-physical networks.

Motivated by the above, we answer the following questions:

- How to securely and efficiently detect the presence of a self-propagating malware (including zero-day attacks) in a network of heterogeneous low-end devices?
- Once malware is detected, how to prevent it from spreading to the entire network and how to securely heal the corrupt devices in a decentralized manner without the intervention from an external trusted party while ensuring minimal overhead?

*Part of the work was done when the author was at IIT Bombay

¹We use the terms "device" and "node" interchangeably in the paper.

As our solution, we present AIRMED², the first decentralized mechanism to recover a heterogeneous network of low-resource cyber-physical systems (CPS) in the presence of self-propagating malware. In addition to device correction, AIRMED further assists in the critical issue of over-the-air code updates. Specifically, it ensures that all devices in the network get updated. We would like to emphasize that, to ensure that our solution remain applicable in a more general sense, we deliberately avoid implementation specific details of IoT devices and study the problem in abstract sense.

At its core, every device in AIRMED performs a periodic self-check of the application that the device is running. AIRMED assumes (readily available) minimal hardware support for the self-check [1, 17, 27]. During the self-check, if a device detects that it has been corrupted, it disables the execution of its application code. Then the device seeks assistance from its neighbors to recover itself with the correct/updated code. We refer such a device as *blank* device. Although, execution of applications are disabled in a blank device, we ensure (ref. §2.2) that it can still communicate with its peers and run the recovery protocol.

Challenges. The resource-constrained nature of low-end devices raises a series of challenges in designing secure and efficient correcting protocols. First challenge is to reduce the trade-off between bandwidth usage and delay in the correction. Specifically, if a device has N neighbors, the procedure of asking each neighbor to transmit the correct application program has a high bandwidth cost. Alternatively, asking the neighbors transmit the correct application in a round-robin manner can lead to long delay in correction. Furthermore, these approach also introduces security vulnerability, as a malicious neighbor can send an incorrect application code to exhaust the bandwidth resources of an honest device.

Second challenge arises due to the fact that each self-check is expensive and involves interrupting normal execution flow. Hence, we want self-checks to be rare, but a rare self-check will allow the malware to stay undetected for longer duration leading to a faster spread.

A third challenge is to efficiently identify the modified portion of the application code to avoid downloading the entire application. This can significantly reduce the bandwidth overhead in devices with large application code. Naive approaches, such as storing a hash of chunks of the application code in a secure memory, increases the size of secure memory. Alternate approach of participating in an interactive protocol as in [23], requires $O(\log z)$ rounds of communication in the worst case to identify a single modified code chunk from a total of z chunk.

Additional challenges include efficient authentication of messages to prevent replay attacks, identifying appropriate and realistic network constraints to ensure that a blank device can communicate with its neighbors. We address all of these challenges in this paper. In summary we make the following contributions:

- We present AIRMED, the first decentralized, secure and a resource-efficient mechanism that ensures recovery of devices in the presence of a self-propagating malware in a heterogeneous network without the intervention of a trusted entity. We also

demonstrate that AIRMED mitigates several critical limitations of prevalent secure device update schemes.

- We perform a rigorous theoretical analysis of various mechanisms used in AIRMED and illustrate their efficiency over naive schemes. We prove that AIRMED guarantees the recovery and update of all the devices and under specific assumptions.
- We present a thorough empirical analysis of AIRMED with multiple topologies using OMNeT++ simulator. Our evaluation illustrates that AIRMED can scale to 1000s of devices, heal 95% network in 10 minutes, and guarantee update of the entire network, while ensuring low overheads.

Organization. We present the System Overview, Threat Model and Required Connectivity in §2. Details about device initialization and network setup are given in §3. §4 presents our detailed design of device correction followed by details of code update in §5. We then, theoretically analyze our design choices in §6. Simulation and Evaluation details are given in §7 and §8. A few related works are described in §9. We finally conclude with a discussion in §10.

2 SYSTEM MODEL

We consider a connected network of N low-end devices, where i^{th} device, n_i , runs a set of applications B_i . Further, we allow devices to store binaries C_i (.bin files) of other applications and transfer these binaries on request from a device connected to it. Let $A_i = B_i \cup C_i$. All devices and the associated binaries are initialized and deployed by a trusted third party \mathcal{O} . As devices often have heterogeneous resources such as memory, bandwidth, and power, based on the resources available at these devices, we classify them into *Low Resource* (LR) and *High Resource* (HR) devices. A LR device only communicates with the devices it is directly connected to; such as devices in its wireless transmission range. Furthermore, LR device only responds to a code request of a neighbor if and only if it already possesses the requested data. In contrast, HR devices can employ fault-tolerant routing algorithms such as Ariadne [21], SAR [44] to communicate with HR devices through a sequence of other HR devices. Also, HR device forwards all kinds of messages as long as it can validate the signature that the message carries. Note that, AIRMED will also work in network with only LR or HR devices as long as the connectivity requirement specified in §2.3 are satisfied.

2.1 Threat Model

A device is called *corrupt* if any of its binaries from A_i is modified by an adversary \mathcal{A} . Similar to existing works, we consider software-only-attacks [5, 8, 17]. Hence, at the application layer, a corrupt device can arbitrarily deviate from the specified AIRMED protocol. Also, \mathcal{A} can drop arbitrary network packets that arrive or leave a corrupt device. Next, based on the malware propagation model, we classify \mathcal{A} into two categories: *Internal* and *External*.

With an internal adversary, we assume \mathcal{A} has, at time 0, corrupted f fraction of devices. Each corrupt device, say n_i , spreads the malware as follows. First, n_i chooses one of its neighbors at random, waits from a time-interval drawn from an exponential distribution with parameter λ_{int} and corrupts the chosen neighbor. If the neighbor is already corrupt, its state remain unchanged. All corrupt devices independently repeat this process for the entire duration they remain corrupt. Intuitively this model captures the

²Goddess of healing (in Irish mythology), known for her prowess in healing those who fell in battle [3].

setting where a corrupt device repeatedly tries to corrupt a randomly chosen neighboring device and in each trial it successfully corrupts the device with tiny probability. Such a model approximately captures the true propagation of a malware [42, 45].

Alternatively, an external adversary corrupts a device by directly connecting to it, and not through one of its neighbors. Specifically, \mathcal{A} first chooses a random device from the network and waits for a time drawn from an exponential distribution with parameter λ_{ext} and corrupts the chosen device. \mathcal{A} repeats this till it is forcefully disconnected from the network. Such an adversary captures proximity attacks where the attacker enters the wireless range of the victim and corrupts it [33].

2.2 Hardware Modules

We next describe the memory organization and communication requirements of devices in AIRMED. This memory organization is already considered in embedded trust anchors such as SMART [17], TyTAN [13], and TrustLite [27]. TrustLite and TyTAN have been implemented on Intel’s Siskiyou Peak research architecture [1].

Memory Organization. The memory of each device is divided into four parts where each part serves a distinct purpose and has different access control. The first part is the Read-Only Memory (ROM) whose contents are fixed during manufacturing and are independent of the application running on the device. ROM stores all procedures required for secure execution of the AIRMED protocol. ROM is executable, and its contents are publicly accessible. One crucial thing to note is that procedures present in ROM can be only invoked starting at designated pre-specified entry points and are executed atomically without any interrupts.

The remaining memory regions are non-volatile and are divided into three parts: code, data, and SecRAM region. code region is executable, stores all application binaries, i.e., A_i of device n_i . The data region is non-executable and is used to store data, and runtime environments such as stack and heap for both procedures in both code and ROM regions. Hence, \mathcal{A} can run modified binaries only if they are stored in the code region.

Lastly, SecRAM (Secure RAM) is non-executable and is inaccessible to procedures present in code. SecRAM is used to store mission-critical mutable data that needs protection from \mathcal{A} . We achieve this property using *Execution Aware Memory Access Control* (EA-MAC) introduced in SMART architecture and later improved by TrustLite [27]. EA-MAC enforces read/write controls depending upon the address of the instruction that is currently being executed. During secure boot of a device, EA-MAC allows a user to specify tuples of memory range say (c, m) with the semantics that memory range m can only be accessed by instructions present in memory range c . For example, TrustLite achieves EA-MAC through its *Memory Protection Unit* (MPU). Figure 1 summarizes the memory organization of AIRMED along with their access permissions.

Communication Stack. In AIRMED, we require blank devices to communicate. We achieve this using the fact that low-end devices are often equipped with separate micro-controller for the networking stack. For example, SimpleLink Wi-Fi CC3000 connectivity module from Texas Instruments is one such commercially available micro-controller with separate networking stack. CC3000 supports IEEE 802.11 b/g and has an embedded IPv4 TCP/IP stack [15]. As

data	Region	read perm.	write perm.	executable
Sec RAM	data	everyone	everyone	no
code	SecRAM	ROM, \mathcal{O}	ROM, \mathcal{O}	no
	code	everyone	everyone	yes
ROM	ROM	everyone	none	yes

(a) (b)

Figure 1: Figure (a) illustrates the memory layout of each device. Table (b) summarizes the read-write permission of each memory region. For example, read and write access to SecRAM is only given to network operator \mathcal{O} , and the code present inside ROM.

networking stack can be isolated from the underlying application or operating system that the device is running, we assume that the networking micro-controller and the software inside it remain functional in a blank device and communicates as follows.

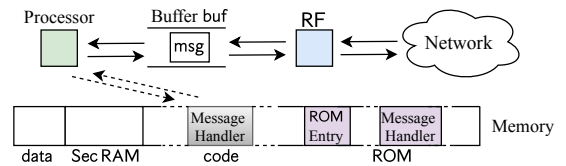


Figure 2: Proposed architecture of a device for enabling a blank device to communicate with the network. The gray message handler belongs to the running application and can be corr. However, the message handler stored inside the ROM is immutable.

Let NIC (Network Interface Card) denote the micro-controller managing the networking stack. When the device is honest, all incoming messages are first handled by the Message Handler of the application or the operating system (OS). Then it is the responsibility of the application’s message handler to invoke procedures from ROM whenever a message is intended for ROM. However, in a blank device, procedures in ROM directly communicate with the NIC module using the secure message handler stored inside ROM. Figure 2 illustrates this architecture.

2.3 Connectivity and Network Requirements

For any given application b , the basic requirement of AIRMED is that a blank device for b should be able to heal itself as long as there exist one honest device in the network that has b . A necessary condition to achieve this is that the induced sub-graph formed by devices with code of b and devices through which they can communicate is connected. To see why, consider the example in Figure 3 containing three devices $\{n_1, n_2, n_3\}$. Devices n_1 and n_3 are HR devices running application b_1 and device n_2 is an LR device running application b_2 . In this network, if n_1 gets corrupted, it cannot correct itself despite the presence of a correct application code at n_3 . This is because device n_2 will refuse to forward messages from n_3 to n_1 .

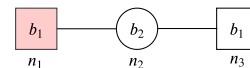


Figure 3: A network of three devices $\{n_1, n_2, n_3\}$ where n_1 and n_3 are HR devices running application b_1 where n_1 is corrupted by \mathcal{A} . n_2 is a LR device running application b_2 .

Generalizing the above, any given network $G = \langle V, E \rangle$ must meet the following requirement. Let $V'_b \subseteq V$ be the set of devices that either runs or stores application b . Let H_b be the set of HR

devices in G that are connected to at least one device in V'_b either directly or through a sequence of HR devices. Let $V_b = V'_b \cup H_b$ and let $G_b \subseteq G$ be the induced subgraph of G with the vertex set V_b . We prove in Theorem 6.4 that AIRMED can correct all applications whose G_b forms a connected component and at least one honest device that stores program of application b exists in G_b under some specific assumptions. In our example in Figure 3, G_{b_1} consisting of device n_1 and n_3 is not connected. Hence, for AIRMED to be most effective, network designer must ensure that G_{b_i} for all i are connected, which can be achieved by first creating a spanning tree among devices running same application and later add more devices to the spanning tree.

2.4 Notations

Let $|M|$ denote the number of elements in a finite set M . If m is a integer (or bit string), then $|m|$ means the bit-length of m . Furthermore, let $\{0, 1\}^\ell$ denote the set of all bit strings of length ℓ .

Attestation. $v \leftarrow \text{attest}(k, d)$ is an algorithm that takes an input k , a bit string d and computes a deterministic digest v of the d . Also, attest guarantees *w.h.p*³ that for any pair of keys k, k' and data d, d' , $\text{attest}(k, d) = \text{attest}(k', d')$ iff $k = k'$ and $d = d'$, where d corresponds to the contents of the code region.

Signature. A signature scheme is a tuple of probabilistic polynomial time algorithms (keygen, sign, ver). $(pk, sk) \leftarrow \text{keygen}(1^\ell)$ where $\ell \in \mathbb{N}$. sk and pk are the signing and verification key respectively, $\sigma \leftarrow \text{sign}(sk, d)$ is the algorithm to sign string d using key sk . Lastly, $\text{ver}(\sigma, d, pk) \in \{0, 1\}$ is the verification algorithm.

Unless otherwise stated, throughout the paper we use $\text{cert}(d)$ to denote $\text{sign}(sk_O, d)$ and verification of $\text{cert}(d)$ implies verification of the signature using pk_O , public key of the operator O .

3 NETWORK SETUP

3.1 Device Initialization

The ROM of each device stores the functions involved in malware detection and device correction, and is initialized at the time of manufacturing. This can be easily extended to the setting where contents of ROM can be modified using a hardware switch present in the device. Hence, O instantiates the remaining regions of memory. Executable files of all applications in A_i are stored in the code region. SecRAM of each device is initialized with pk_O , a freshly generated asymmetric key pair (pk_i, sk_i) unique to n_i along with the certificate $\text{cert}(pk_i)$. For each application in A_i , O stores their version numbers $\text{ver}(A_i)$, $\text{cert}(\text{ver}(A_i))$, and $\text{cert}(A_i)$ in SecRAM. The reason behind storing these certificates is to allow the device to prove correctness of its code to other devices in the network. Lastly, O also initialize each device with the self-check rate λ , the maximum allowable self-check rate λ_{\max} , and the minimum allowable self-check rate λ_{\min} . A detailed description of these self-check rates are given in §4.

Once initialized, each device locally generates a cryptographic symmetric key k_i , attest key ak_i , and a sequence key q_i as uniformly distributed random numbers in $\{0, 1\}^\ell$. The attest key is

³For any security parameter $\ell > 0$, an event happening with high probability *w.h.p* implies that the event happens with probability $1 - o(1/\text{poly}(\ell))$. Here $\text{poly}(\ell)$ refers to class of all polynomials with parameter ℓ .

used to compute attestation over the contents of code, and q_i is used to prevent replay attacks. Let v_i be the output of the attestation procedure. n_i next generates a set of keys L , of size $\kappa = |L|$, which is used to initialize a bloom filter F of size $\mu Z/t$. Here Z is the size of the code region whose contents are divided into chunks of size t bits each. Refer [26] for more details of bloom filters.

3.2 Device Rendezvous

Every device in the network periodically announces itself to other devices in its transmission range by broadcasting a hello message. On hearing a new device, say n_j with public key pk_j , device n_i rendezvous with it to validate each other's certificate $\text{cert}(pk_i)$ and $\text{cert}(pk_j)$. On successful validation, they securely exchange their keys (q_i, k_i) and (q_j, k_j) . As a device rendezvous with other devices only once, the key exchange mechanism can be realized using the key-exchange scheme of TLS 1.3 [12]. Let N_i be the set of all devices in n_i 's transmission range with whom n_i has rendezvous with, hereon we refer to the devices in N_i as the *neighbors* of n_i . Hence at the end of rendezvous, n_i will have a set of $\{k_j, q_j\}_{\forall j \in N_i}$. Note that, in our scheme, each device shares the same key with all its neighbors. We do this primarily for efficiency. This can be easily extended to establish a unique symmetric key between each pair of devices. Table 1 summarizes the memory contents of each device at the end of initialization and rendezvous.

Table 1: Memory content of a device after initialization and device rendezvous phase.

Region	Manufacturing/Initialization	Rendezvous
SecRAM	$pk_O, (pk_i, sk_i), \text{ver}(A_i), \text{cert}(A_i), \text{cert}(pk_i), \text{cert}(\text{ver}(A_i)), \lambda_i, \lambda_{\min}, \lambda_{\max}$	$\{k_j, q_j\}$
	$k_i, q_i, (ak_i, v_i), F$	
code	A_i	
ROM	$\text{selfcheck}(), \text{attest}(), \text{sign}(), \text{rectify}(), \dots$	

4 DESIGN OF AIRMED

At a very high-level, correction of a corrupt device in AIRMED involves the following steps. Each device periodically initiates a self-check procedure to detect whether it is corrupt or not. In case the device is found to be corrupt, its hardware disables execution from its code region. Then the device queries its neighbors for a correct application code. We next look at each of these procedures in detail.

4.1 Detecting Malware

Every device performs periodic self-check with the time interval between two consecutive self-checks chosen from an exponential distribution with parameter λ . As expected value of exponential distribution with parameter λ is $\frac{1}{\lambda}$ [32], the expected time between two consecutive self-check is $\frac{1}{\lambda}$. We pick time intervals from an exponential distribution due to their memoryless property [32]. As the rate of propagation of malware depends crucially on the time a device remains infected, memoryless self-checks will prevent \mathcal{A} from strategically infecting devices to increase the duration for which the device remains corrupt. Furthermore, memoryless self-checks prevents a mobile adversary from evading detection by uncorrupting a infected nodes just before the next self-check [31].

Let $\delta \leftarrow \exp\{\lambda\}$ be one such realization of the time interval. Starting from last self-check, δ is decremented by one in every clock cycle. When δ reaches zero, the processor generates a hardware interrupt. On this interrupt, the processor pauses the running application, records the run-time state of the application in a non-volatile memory and invokes `selfcheck()` procedure from ROM. Also, all interrupts are disabled to allow atomic execution of `selfcheck`.

Procedure `selfcheck()` first invokes procedure `attest()` with its input as ak_i and entire contents of the code region. Let v'_i be the attestation result. If v'_i equals to v_i , i.e., the contents of code are not tampered, `AIRMED` increments the expected wait time between self-checks, that is $\frac{1}{\lambda} = \frac{1}{\lambda} + 1$ as long as it does not exceed a pre-defined upper bound. In other words, it sets λ to $\max\{\lambda_{\min}, \lambda/(\lambda + 1)\}$. Next, interrupts are enabled and the control is given back to the application. On the contrary, $v'_i \neq v_i$ implies modification of the application code. In such a situation, instead of resuming the application, `selfcheck` sets a hardware bit to make the code region non-executable, and invokes `rectify()`, another secure procedure from ROM. The pseudocode of `selfcheck()` is given in Algorithm 1 where we use `[code]` to refer to the contents of the code region.

Malware localization. Once the tampering has been detected, the next goal is to identify the tampered region of the code to avoid downloading the entire application program. A naive approach of dividing the entire `[code]` into chunks of size t and storing hash of each chunk in SecRAM has high memory usage. Specifically, if $Z = |[code]|$, then this approach would require storing $\ell Z/t$ bits of additional storage in SecRAM, where ℓ is the size of the output of the hash function.

In `AIRMED` we reduce this storage overhead through novel use of bloom-filters. Recall from (§3.1), that a $\mu Z/t$ bit long (for small constant μ) bloom filter F is initialized with partitions of `[code]` using the set of secret keys L . Hence, to localize the malware, `rectify()` finds all chunks that are absent in F . The idea is, since \mathcal{A} is unaware of keys in L , the chunks modified by the adversary will most likely be absent in the F and hence will be detected by `rectify()`. For example, in Figure 4, adversary modifies i^{th} chunk to c'_i , which is absent in the filter F . As a result, instead of the entire application code the blank device will query its neighbors only for the chunks that are marked as absent in the bloom filter.

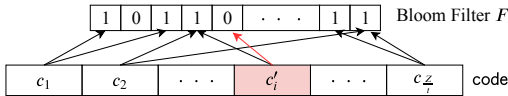


Figure 4: Adversary modifies i^{th} chunk to c'_i which is absent from the filter F .

However, since bloom filters have non-negligible false positive rates, it is possible (albeit rarely) that `rectify()` fails to identify all the modified chunks. In such situation, the blank device downloads the entire application program. Also, we keep t and number of keys in L parameterizable that can be picked for any desired false positive rate. For example, with $Z = 16384$, i.e., 16KB of executable memory, which is typically the case in MSP430 micro-controllers [15], $\mu = 8$, $|L| = 4$, and $Z/t = 32$, we show in §8.3 that a blank device will download the entire application program less than 2% of the time. Refer to [32] for detailed analysis of false-positives in bloom filters.

Once the corrupted chunks has been identified, interrupts are re-enabled. We call a device with disabled execution as a *blank* device. Recall (ref. §2.2), in all blank devices all incoming messages are directly handled by functions in ROM (ref. §2.2).

4.2 Correcting blank Devices

The basic idea of correction is that once a device n_i becomes blank, it asks one of its neighbors to send the correct version of the compromised code along with the certificate from O . n_i on receiving these chunks validate their correctness by checking the certificate from O . On successful validation, it installs them in its code region and starts normal execution of the application program. Further, in scenarios where devices in N_i are running different versions of the code, it is desirable to download the most recent version of the application among all available versions. Here we are implicitly assuming that recent versions of application programs have a higher version number.

A naïve approach is to send a message to each neighbor and request for the necessary chunks of code. On receiving the application programs from each neighbors, n_i locally identify the highest version, validates it and then installs it. This approach is bandwidth inefficient as it requires each neighbor to transmit all codes, which might be relatively large in a resource constrained setting.

An alternate approach is to first ask neighbors for the version number of application b they are running, and then request the neighbor running the highest version to send the code. Although this approach is bandwidth-efficient, it has several limitations. First, this approach does not protect n_i from requesting code from a malicious neighbor that might deny or delay the response to the code request by merely dropping or delaying the code request message. Further, in the case of dense network the cost of transmitting so many version messages could still be overwhelming. Also, none of these approaches prevent a corrupt device from sending spurious version and code request to honest devices and drain their bandwidth and computation resources.

Our Approach. Let $\Pi \subseteq [Z]$ denote the set of corrupt chunk indices at the blank device n_i . For simplicity, let us assume that all of the corrupted chunks belong to a single application b with its version being $z_i = \text{ver}(b)$. Also, let us assume that Π includes all modified indices, i.e., there is no false positive due to the bloom filter. Let $N_i^{(b)} \subseteq N_i$ denote the set of devices among neighbors which are in G_b , i.e., the induced subgraph of G for application b (ref. §2.3). We assume that n_i is unaware of the identities of devices in $N_i^{(b)}$.

To request correct code, n_i broadcast to its neighbors a message MSG_{req} with $\langle \text{req}, \text{ttl}, q_i, |N_i|, z_i, b, \Pi \rangle$ as its payload. Unless otherwise stated, we assume that all messages are tagged with a message *Message Authentication Code*, source of messages can be established for every message transmitted in the wireless range, and sequence number q_i is incremented by n_i after every message. Tag `req` in message payload specifies that this message is to request for binaries. Sequence number q_i assists devices in N_i to establish validity and freshness of MSG_{req} .

Adaptive self-check rate. Each honest device $n_j \in N_i$ on receiving MSG_{req} first updates its self-check rate as:

$$\lambda \leftarrow \mathbb{1}_{\text{ttl} > 0} \min\{2\lambda, \lambda_{\max}\} + \mathbb{1}_{\text{ttl} \leq 0} \lambda \quad (1)$$

where $\mathbb{1}_x$ is a indicator function which is equal to value 1 if x is true and 0 otherwise. ttl in the message payload is the parameter to limit broadcast of device corruption message. Additionally, when $\text{ttl} > 0$, device n_j broadcasts a warning message to all its neighbors, i.e., devices in N_j informing about corruption of n_i with parameter $\text{ttl} - 1$. Similar to devices in N_i , devices in $N_j \setminus N_i$ updates their self-check rate according to equation 1 and recursively forwards it to their neighbors as long as ttl reaches zero. Figure 5 (a) and (b) illustrates the self-check rate of neighbors of n_3 , before and after n_3 broadcasts MSG_{req} with $\text{ttl} = 1$.

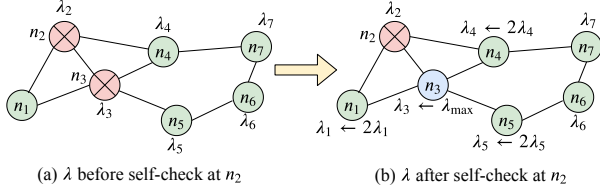


Figure 5: Self-check rate of neighbors of a device n_3 before (a) and after (b) n_3 broadcasts MSG_{req} with $\text{ttl} = 1$. As a result, honest neighbors n_1 , n_2 and n_5 updates their λ using equation 1. Also, n_3 sets its own self-check rate to λ_{max} .

Code transmission with random-backoff. To address the issue of redundant code transmission, each neighbor n_j of a blank node n_i , performs a uniform random-backoff with backoff delay τ_j as:

$$\tau_j = \max\{\Delta - (z_j - z_i), 0\} |N_i| \theta + \lfloor \mathcal{U}(0, 1) |N_i| \rfloor \theta \quad (2)$$

where Δ estimate of maximum difference in version numbers among devices running a particular application. Similarly, θ is a protocol parameter denoting the approximate upper bound on time required to transmit the requested chunks, z_j is the version number of b at n_j , and $\mathcal{U}(0, 1)$ is a value chosen uniformly randomly between $(0, 1)$. The intuition behind this approach is two fold: *first*, we prioritize responses from devices running a higher version of the same application; *second* among devices running the same version of the application, we aim to spread the time when these device transmits the requested chunks. Device n_j only starts the timer if $z_j \geq z_i$, otherwise n_j simply discards the message. Figure 6 illustrates the the distribution of transmission time at neighbors of n_1 . Pseudocode in 2 describes the steps taken by each device in N_i .

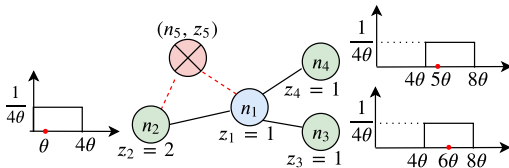


Figure 6: Distribution of time at which neighbors of blank node n_1 , i.e., $N_1 = \{n_2, n_3, n_4, n_5\}$ transmits the requested chunks of code. Here, $\Delta = 1$, $|N_1| = 4$, node n_5 is corrupt, version of n_2 , i.e., $z_2 = 2$ and all remaining node has version 1. Red dot on the time axis in each graph, is one realization of the transmission time.

Without loss of generality, let $n_j \in N_i^{(b)}$ be the honest device with smallest back-off interval τ_j among all honest devices in $N_i^{(b)}$. Once τ_j expires, n_j sends a single chunk to n_i and waits for an acknowledgement from n_i . On receiving the acknowledgement message from n_i , n_j sends the remaining chunks. If more than one

honest device simultaneously sends the first chunk, n_i sends acknowledgement to only one of them. We present a detailed analysis of such scenarios in §6.2.

Stream Signatures. If we use a signature scheme in which a blank device n_i must receive all chunks before verifying their signatures, it will allow an adversary to waste a lot of bandwidth by sending invalid chunks and n_i will not know they are invalid till the very end. We mitigate this attack using on-line variant of stream signature introduced in [19]. In stream signature, the signer \mathcal{O} , signs first chunk and embeds in each chunk c_i the hash of the next chunk c_{i+1} . Figure 7 illustrates this. As a result, a bogus chunk can be detected immediately.

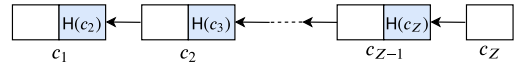


Figure 7: In stream signature messages are divided into chunks and each chunk (except the last chunk) contains the hash of the next chunk, i.e., c_i contains $H(c_{i+1})$. The signer only signs the c_1 .

Lastly, once n_i receives all chunks in Π , it broadcasts a MSG_{done} to its neighbors indicating that it has successfully corrected itself. Honest neighbors on hearing MSG_{done} cancel their back-off timers (if any) corresponding to n_i 's code request. Alternatively, if n_i do not receive all the correct chunks within time $\Delta |N_i| \theta + |N_i| \theta$, n_i rebroadcasts MSG_{req} with the updated Π after a time delay of δ drawn from $\exp\{\lambda\}$. Such as situation could possibly arise if either all devices in $N_i^{(b)}$ are running a lower version of b , or they are in blank or corrupt state. Algorithm 3 presents the pseudocode for handling a response to MSG_{req} message.

Fast Correction. AIRMED also enables fast correction of a cluster of blank devices. With solely the method just described above, if the nearest honest device is r hops away, correction of d_i takes in the best case an expected time of r/λ_{min} . To enable faster correction, whenever a device n_j is corrected, it immediately broadcasts a message containing information about the corrected code, its version number, and the corresponding certificates. On hearing this message, blank device seeking the appropriate binaries can actively request it from device n_j . As a result, the corrected binaries spreads through the network much faster without waiting for the timers of blank devices to expire.

5 UPDATE OF APPLICATION BINARIES

So far we have only looked at how a compromised device self-corrects itself with the help of its neighbors. We now consider the behavior of the whole network that is running the AIRMED protocol specifically in situations where \mathcal{O} updates the application program executed with newer versions. To expound AIRMED's applicability for updating binaries in a network of low-end devices we consider a prevalent update technique motivated from [9, 28, 35], study it in our threat model and show its limitations. We then make minor modifications to the AIRMED protocols described so far, and show that AIRMED when combined with this network update technique overcomes these limitations. For brevity we will only focus on the network G_b for a specific application b . This can be easily extended to the entire network. Also, each newer version comes with a monotonically increasing version number.

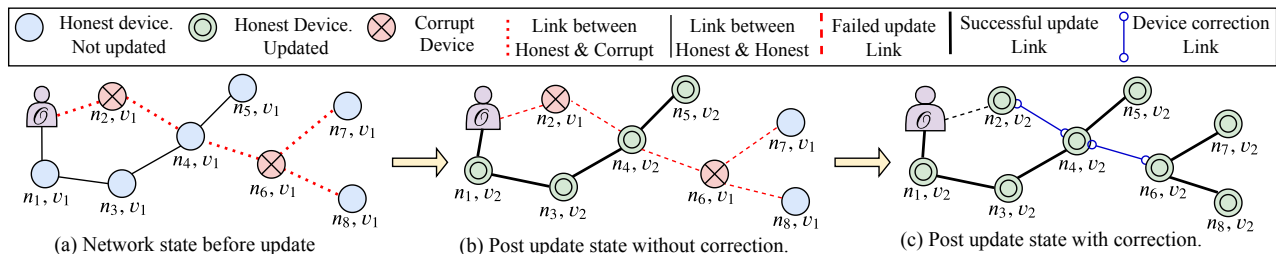


Figure 8: code update in a network of 8 devices $\{n_1, \dots, n_8\}$ with device n_2 and n_6 corrupt prior to update (a). Initially all device run the same version v_1 of the application. Let $v_2 > v_1$ be the updated version, then without a correction mechanism only $\{n_1, n_3, n_4, n_5\}$ will be updated (b). However, when deployed along with AIRMED the entire network will get updated once n_2 and n_6 perform self-check (c).

Consider the following recursive swarm update mechanism of [9]. Here O first must find one device which is honest and then update it with a newer version of the application. Finding an honest device is important because a corrupt device can simply drop the update messages. This originator device then updates its neighbors and so on to form a virtual update tree.

This scheme has several shortcomings. First, in case a large fraction of devices are corrupted, O may have to contact many devices to find one honest one. Hence it allows malware to spread for longer duration. Second, the above approach can only update devices connected to the O through a sequence of honest device and all other devices may still remain corrupted.

Suppose we use AIRMED along with this recursive update procedure. Even if a large number of devices are corrupt, they will become blank and then get corrected over time. Thus O has a higher chance of encountering a device which is either blank or running a correct application. In fact, if O is in contact with κ devices (say in wireless communication range of them), then from elementary probability theory, the expected time for at least one of them to become blank is at least $1/((\kappa + 1)\lambda_{\min})$.

We now show how the second problem of the update scheme in [9], namely the inability of the update to reach any corrupted device, is solved. The update propagates on an honest virtual tree as before. Consider a corrupt device which has a neighbor in this tree. After it performs a self-check it becomes blank and then obtains the latest version from its neighbors. We now make a minor modification to AIRMED. This device then acts like a new root and propagates the latest version to its neighbors who are honest but do not have the latest version. This increases the size of the virtual tree running the latest version, until the virtual tree encompasses the entire G_b . This is illustrated in the transitions of Figure 8.

Let the network shown in Figure 8(a) be the G_b consisting of devices $\{n_1, \dots, n_8\}$ for application b with v_1 as the current version. Let n_2 and n_4 be the corrupted devices. With this initial state of the network, O will successfully initiate the update procedure with at-most two trials. Let $v_2 > v_1$ be the newer version of b . Without any correction mechanism the update will fail to reach honest device $\{n_7, n_8\}$. Also the corrupt devices will not be updated as well. Figure 8(b) illustrates this.

However, in AIRMED, as soon a corrupt device performs a self-check and detects that it has been compromised, it will download the updated code from one of its neighbors. Further, it will forward the information about the newer update to all the devices in its

neighborhood that are running an obsolete version of the application. Stated differently, when n_6 corrects itself it then behaves as a new originator and updates n_7 and n_8 as shown in Figure 8(c). This is analogous to a temporary pause of the original update procedure due to adversarial devices in the path and its resumption later as the devices enter the blank state as a part of the protocol.

6 ANALYSIS

6.1 Secure Memory Cost

Recall (ref. §3.1), for malware localization, AIRMED uses a bloom filter of size $\mu Z/t$ and $|L|$ keys for input to the hash function of the bloom filter. Hence, AIRMED stores $\ell|L| + \mu Z/t$ bits of information in secure memory. Where as, naive approach of storing hash of each chunk would have required $\ell Z/t$ bits of memory. Next, with the help of Table 1, we evaluate the size of SecRAM required to store the remaining information for a single application. This can be easily extended to multiple applications. Each device n_i stores two asymmetric public key, pk_O and pk_i , one asymmetric private key sk_i . Let $|pk_O| = |pk_i| = |sk_i| = 1024$. If each certificate is of size 256 bits, each device stores one certificate for its public key and two certificates for each application. Also we use same number of bits for all three self-check parameters, i.e., $|\lambda| = |\lambda_{\min}| = |\lambda_{\max}| = 32$. Similarly, let $\ell = |k_i| = |q_i| = |ak_i| = |v_i| = 128$. Lastly, for each of its neighbor in N_i , a device needs to store $256 = 2 \times 128$ for the shared symmetric key and the sequence number. Summarizing the above,

$$|\text{SecRam}| = 3|pk| + (4 + |L|)\ell + 3|\text{cert}| + \frac{\mu Z}{t} + 3|\lambda| + 2|k||N_i| \quad (3)$$

6.2 Communication Cost.

The first major source of communication is due to the fact that a blank device in AIRMED only requests for the modified chunks. However, as bloom filter has non-negligible false-positive rates and it is possible (albeit rarely) that the bloom filter fail to localize the malware. Thus for any given Z , t , μ and L , we compute the expected number of chunks a blank device needs to download to correct itself.

Let κ be the number of chunks modified by the adversary. Since, the bloom filter keys are inaccessible to the attacker, from elementary cryptography, the attacker can not make strategic modifications to evade the bloom filter check [26]. Hence, we assume modifications of these chunks to be arbitrary. Let p be the false positive rate for a single chunk; then with the above assumptions, $p = (1 - e^{-|L|/\mu})^{|L|}$. Refer to [26] for more details.

THEOREM 6.1. *Assuming hash functions are ideal, if an adversary corrupts κ chunks from a total of Z/t chunks in a device which uses bloom filter scheme of [26] with $\mu Z/t$ bit filter and $|L|$ hash functions, then the probability that the blank device download the entire code is:*

$$\Pr[\text{download entire code}] = 1 - (1 - p)^\kappa \quad (4)$$

Also, expected number of chunks the blank device will download is:

$$\frac{Z}{t} (1 - (1 - p)^\kappa) + \kappa (1 - p)^\kappa \quad (5)$$

PROOF. Whenever, the device all κ modified chunks, it only downloads κ chunks. This gives us the second term of equation 6. Alternatively, even with a single false positive among κ chunks, the device downloads all Z/t chunks. Combining this with equation (4), we get the first term of our result. \square

The next source of communication improvement is due to the random back-off procedure used for reducing the number of neighbors that transmit the requested chunks. The following theorem (proof in Appendix) illustrates that the expected number of neighbors that will transmit the requested chunks.

THEOREM 6.2. *If a device has m neighbors, then the expected number of neighbors that transmits the requested chunks are*

$$\sum_{j=1}^{m-1} \sum_{k=1}^m \left(\frac{k \binom{m}{k} (m-j)^{(m-k)}}{m^m} \right) + \frac{m}{m^m} \quad (6)$$

6.3 Recoverability

Next, we theoretically argue that AIRMED recovers and guarantees update of the entire network in the presence of both internal and external adversary under specific assumptions (Proofs in Appendix C). For an heterogeneous network $G = \langle V, E \rangle$ of devices, we define the graph $G_b \subseteq G$ for application b as:

Definition 6.3. For any given application b , let $V'_b \subseteq V$ be the subset of devices that either runs or stores the application b . Let H_b be the set of HR devices in G that are connected to at least one device in V'_b either directly or through a sequence of HR devices. Let $V_b = V'_b \cup H_b$. Then G_b is the induced subgraph of G due the vertex set V_b .

THEOREM 6.4. *If G_b is connected and no additional device gets corrupted after a given time t_0 and there exists at least one honest device running or storing application b at time t_0 , then AIRMED corrects all devices in G_b .*

THEOREM 6.5. *If G_b is connected and if the update patching the vulnerability is successfully initiated by \mathcal{O} in at least one device in G_b , then AIRMED guarantees update of the entire network in the presence of both internal and external adversary.*

7 SIMULATION

Since the cost of evaluating AIRMED on a large scale network consisting of thousands of device would be high, we test AIRMED by simulating it in OMNeT++ version 5.5.1 [4]. We simulate both internal and external malware propagation with update scheme of [9].

Network Topology. We test AIRMED on three different topology with approximately 1024 LR devices each, with all devices running the same application. Our first topology is a connected *Mesh* wireless network of 1024 devices spread uniformly across an area of 4 km \times 4 km. Each device has a wireless transmission range of 200 meters around it. The intent behind this topology was to capture scenarios such as the ad-hoc deployment of sensor network that are ubiquitous in Military application, agriculture, forest fire monitoring system, etc. [24, 25, 40]. The remaining two topologies we simulate are Binary and Ternary tree. We pick them to capture Industrial IoT, Building management etc [16]. In all the above topologies, we use the same 20 ms average transmission delay between each pair of connected devices, as it is the average value in ZigBee sensor networks [38]. Lastly, during an update, \mathcal{O} connects to a randomly chosen device and update it with a newer version.

Internal Adversary. To evaluate the effect of internal adversary \mathcal{A}_{int} , for each the topology we corrupt $f = 30\%$ of the randomly chosen devices to begin with. We also vary the malware propagation rate, λ_{int} and the number of hops in the limited broadcast to inform neighboring device about the presence of an adversary in the network. For each topology, we consider two different initial configuration depending upon the positioning of the corrupt devices. Namely, we consider configuration C_0 and C_1 . In C_0 , the initial fraction of corrupt devices are distributed uniformly across the entire network. In C_1 , the corrupt devices form a single island, i.e., corrupt device form a single connected network. To create these initial configurations, we first enumerate all the device. For configuration C_0 , we then pick $f|N|$ unique device uniformly randomly. For C_1 , we first select a device uniformly at random and starting at this chosen device; and then we pick up to $|N|f$ device by performing breadth-first-search.

External Adversary. External adversary \mathcal{A}_{ext} corrupts uniformly randomly independent of the devices corrupted in the past. Unlike \mathcal{A}_{int} , we evaluate the effect of \mathcal{A}_{ext} starting from network with all honest device. Also, we disconnect, i.e., disallow \mathcal{A}_{ext} from corrupting more devices after a specified period. In practice, one can disconnect \mathcal{A}_{ext} from further corruption by isolating it from the internet. Let λ_{ext} be the corruption rate of \mathcal{A}_{ext} . \mathcal{A}_{ext} corrupts a randomly chosen device after intervals drawn from a exponential distribution with parameter λ_{ext} . Also, once \mathcal{A}_{ext} is disconnected from the network, no additional device gets corrupt.

Correction and Update For all our simulations, we use initial $\lambda = 1/100$, i.e., the average inter-arrival time between two consecutive self-check is 100 seconds. To evaluate the network behavior with an adaptive self-check rate, we run all our experiments with $\text{ttl} = 0, 1, 4$. Note that, $\text{ttl} = 0$ is the baseline situation where neighboring devices do not increase their self-check rate on hearing warning messages from their neighbor. In all these experiments we keep λ_{max} and λ_{min} to be $1/100$ and $1/400$, respectively.

8 EVALUATION

All the results presented in this section corresponds to simulation of AIRMED for 1000 seconds. These results are averaged after 10 simulations with distinct randomness seed. Unless otherwise stated, updates in the presence of \mathcal{A}_{int} and \mathcal{A}_{ext} are scheduled at 500 and

700 seconds respectively, from the start of the simulation. \mathcal{A}_{ext} is disconnected at time 300 seconds from the start of the experiment.

8.1 Internal Adversary

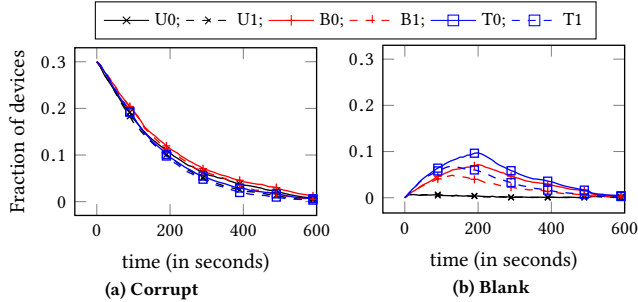


Figure 9: Fraction of (a) corrupt and (b) blank devices in the presence of \mathcal{A}_{int} with $f = 0.30$ and $\lambda_{\text{int}} = \lambda_{\text{max}}$ for configuration C_0 . Here B0 and B1 refer to Binary Tree topology with $\text{ttl} = 0$ and $\text{ttl} = 1$ respectively. Similarly, we use U0,U1 and T0,T1 for Mesh and Ternary tree topology respectively.

Varying Network Topology. Figure 9a and 9b illustrates the fraction of corrupt and blank devices respectively at any given time for all three network topologies with configuration C_0 , initial corrupt fraction $f = 0.30$, and $\lambda_{\text{int}} = \lambda_{\text{max}}$. Notice that, for all three topologies, the fraction of corrupt devices starts decreasing almost from the start of the simulation. This is because the effective malware spread rate in these topologies are lower than λ . In Binary tree topology, approximately half of the initial corrupt devices will be leaf devices. All these devices only have one neighbor, and also often this neighbor is shared between multiple corrupt devices. Hence, these leaf devices will repeatedly try to corrupt an already corrupt device. A similar situation arises in Ternary tree topology as well. Further, the rate of reduction of corrupt devices closely follows the tail of an exponential distribution. This is due to exponential distribution of interarrival between consecutive self-checks. Notice that the fraction of blank node in Mesh topology remains almost zero for the entire duration, whereas it first increases in the tree topologies and then decreases. Again, this is because approximately half the devices in tree topologies have only one neighbor. Thus these nodes cannot self-correct themselves unless their neighbor corrects itself. Also, as expected, we observe a lower fraction of corrupt and blank devices for $\text{ttl} = 1$ as devices will perform more frequent self-checks and will recover sooner.

Adaptive self-check with varying Configuration. Figure 10 represents the time required for 95% of the network to become correct, starting with 30% of devices being corrupt for varying $\text{ttl} = 1, 2, 4$. Devices in C_0 (solid lines) correct themselves quickly than devices in C_1 (dashed lines). This is because in C_1 , at any given time, only devices positioned at the edge of the corrupted island can correct themselves whereas devices positioned inside the corrupt island need to wait for their neighbor devices get corrected. Interestingly, non-zero ttl introduces a larger drop in correction time in C_1 . This is because corrupt devices at the boundary of the corrupt island share a considerable fraction of honest neighbors. Hence, these honest devices perform faster self-checks as they will

update their self-check period more frequently. We do not see major improvements from $\text{ttl} = 1$ to $\text{ttl} = 4$ due to the local nature of malware propagation. One exception here is the Mesh topology in C_0 . This was expected as each device in Mesh topology has a higher number of neighbor and hence higher ttl cautions nodes farther apart to update their self-check rate.

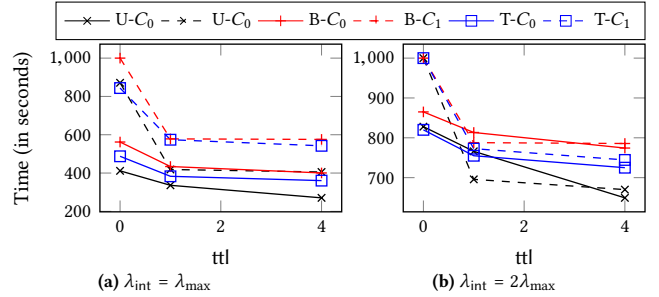


Figure 10: Time when 95% of the devices in the network becomes correct starting from an initial fraction of 30% corrupt devices in Binary (B), Mesh (U), and Ternary (T) topologies for varying ttl . Solid and dashed lines corresponds to C_0 and C_1 respectively.

Update with different Configuration. Figure 11 illustrates the fraction of updated device over time in all topologies for configuration C_0 and C_1 with $f = 0.30$. In all the experiments, eventually, almost all devices get updated. In both C_0 and C_1 , update in tree topologies takes longer because, a single corrupt device can temporarily stop updates in its entire subtree. Update in tree topology for C_0 takes longer time than C_1 , because corrupt devices are more evenly spread across the network and hence code update temporarily halts more often in C_0 . Ternary tree topology has a faster update than Binary tree due shorter tree height and large average number of neighbors.

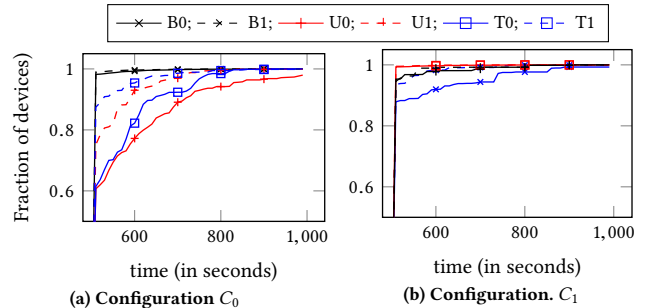


Figure 11: Fraction of updated devices in the presence of an internal adversary with $f = 0.30$, malware spread rate $\lambda_f = \lambda_{\text{max}}$ for Binary (B) tree, Ternary (T) tree, and Mesh (U) network topology. Figure (a) and (b) corresponds to C_0 and C_1 respectively. Solid and dashed lines correspond to $\text{ttl} = 0$ and $\text{ttl} = 1$ respectively.

8.2 External Adversary

Varying network topology. Red and black plots in Figure 12a and 12c illustrates the fraction of corrupt devices for Mesh and Binary tree topology with $\lambda_{\text{ext}} = \lambda_{\text{max}}, 2\lambda_{\text{max}}$ respectively. We omit the results for the Ternary tree as it is very similar to the results of Binary tree topology. For both topologies, the fraction of undetected corrupt device increases approximately until 100 seconds

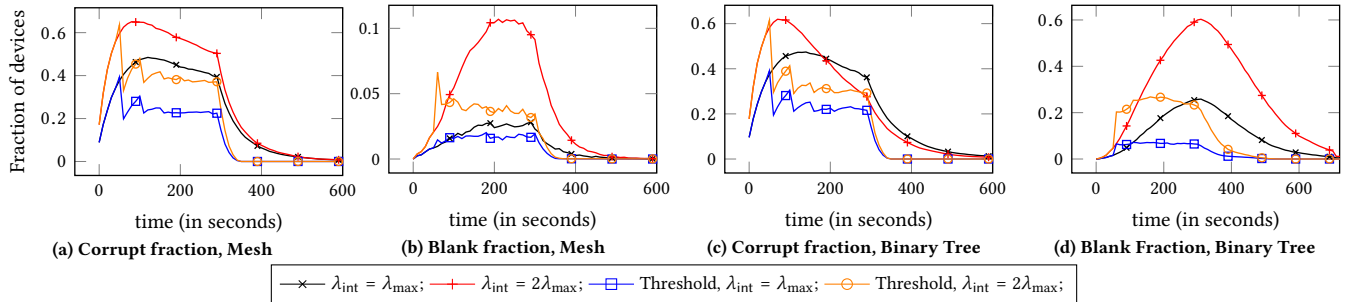


Figure 12: Fraction of corrupt and blank device in Mesh and Binary Tree topology in the presence of an external adversary \mathcal{A}_{ext} . Solid lines corresponds to the adaptive case with $\text{ttl} = 1$ and dashed lines corresponds to non-adaptive case, i.e., $\text{ttl} = 0$. Plots for the situation where the interarrival time between two consecutive self-checks are

and then gradually starts decreasing. This is because we initialize $\lambda = \lambda_{\text{max}} = 1/100$. Interestingly, after 100 seconds, although the adversary is corrupting additional devices, the fraction of corrupt nodes decreases even for $\lambda_{\text{ext}} = 2\lambda_{\text{max}}$. This is because adversary randomly chooses device for corruption and since more than 50% of the devices are already corrupt or blank by time 100s, the effective corruption rate is lower than λ_{max} .

The fraction of blank devices is higher in Binary tree topology because blank devices in Binary tree have fewer neighbors, and hence they remain blank till one of their neighbor corrects itself. Alternatively, in Mesh topology average number of neighbors per device is higher, which increases the likelihood of one honest neighbor at any given time. This also explains the rapid decrease in fraction of corrupt device in Binary tree topology. As blank devices are immune to corruption, the probability of corrupting an honest device is lower in Binary tree topology. Once \mathcal{A}_{ext} is disconnected from the network, i.e., after 300s, the rate of reduction in fraction of corrupt device follows the tail of exponential distribution.

Varying Spread Rate. Black plot in Figure 12 corresponds to $\lambda_{\text{ext}} = \lambda_{\text{max}}$ and red plot corresponds to $\lambda_{\text{ext}} = 2\lambda_{\text{max}}$. As expected with higher λ_{ext} , a higher fraction of devices gets corrupt. Also, for the same reason, the fraction of the correct device is lower for the lower corruption rate. Interestingly, the fraction of corrupt devices is higher in Binary tree topology after 200s for $\lambda_{\text{ext}} = 2\lambda_{\text{max}}$. As discussed earlier, this is due to the higher fraction of blank devices in the network which reduces the effective malware spread rate.

Thresholding self-check rate. So far we have only considered the scheme where the interarrival time between consecutive self-checks at honest devices are drawn from an exponential distribution with parameter λ . An issue with this approach is the unbounded interarrival time. Thus, we evaluate AIRMED with the modification where we upper bound the self-check period by 50 seconds, i.e., $\delta \leftarrow \min\{\exp\{\lambda\}, 50\}$. Blue and orange plots in Figure 12 illustrates this results in the presence of \mathcal{A}_{ext} . Observe that, thresholding reduces the fraction of corrupt and blank devices. This is because, devices are performing frequent self-checks, hence detecting the malware earlier. But this comes at the cost of higher energy usage. Also, for both Mesh and binary tree topologies, at time instants that are multiples of 50, a large number of devices detects and hence corrects themselves. Interestingly, the fraction of corrupt device

does not reach zero at time instants because additional devices whose first self-check interval was less than 50 gets corrupted.

8.3 Performance

As we describe in §6.1, our bloom filter based approach requires $\ell|L| + \mu Z/t$ bits of SecRAM space in contrast to $\ell Z/t$ bits of space using the naive approach. Therefore, for $Z = 16384$ Bytes, i.e., 16 KB which is typically the case with Texas Instrument’s MSP430 micro-controllers [15], for $t = 256$ Bytes, $|L| = 4$ and $\mu = 8$ we will only require 128 Bytes of additional space in SecRAM. This gives us an $8\times$ improvement over the naive system with $\ell = 128$. Moreover, by substituting these numbers in equation (5), we get that the expected number of chunks, a blank device needs to download for $\kappa = 4$, i.e., when adversary modifies content of four chunks, is ≈ 10 . This is $6\times$ better than the naive scheme of downloading all the chunks. Lastly, using equation (6), we get that the expected number of the honest neighbors who will transmit the requested chunks for different values of m , the number of honest neighbor in the worst case are:

# neighbors, m	2	5	10	20
$E[\# \text{ neighbors to transmit code}]$	1.50	1.57	1.57	1.58

This shows even in dense network, in expectation, less than two neighbors will end up transmitting the requested chunks. This is significantly better than all the naive approaches.

9 RELATED WORK

AIRMED falls into the genre of Device Swarm Security. While our work focuses on correction and updation in the presence of an adversary, most of the previous works looked only at only attestation in the presence of an adversary or updation with no adversary.

Proposals such as [5, 8, 14] assume a *Single External Verifier* to carry out swarm attestation while others [22, 43] use a *Decentralized* approach where each member device is attested by a genuine node in its neighborhood. Ambrosin M. et al. designed a collective attestation scheme for IoT swarms for Highly Dynamic Swarm Topologies [6]. These methods do not address updating or correction of code, however.

In SAFE^d [41], a pair of embedded devices in a swarm attest to each other without the need of an external verifier. Similar to [43], SAFE^d also removes a single-point-of-failure issue by allowing swarm members to coordinate and self-protect the underlying network. The SAFE^d network forms multiple overlays among swarm

members that replicate proofs indicating the correctness of prover devices. Recently, Ibrahim et al. proposed HEALED [23], a new attestation scheme capable of detecting corrupt device and healing upon compromise. Every corrupt device in HEALED, interact with honest device to localize modified memory regions. This approach requires $O(\log z)$ rounds of communication to identify a single corrupt region for a application program of size z . Also, none of the above approaches consider propagating malware. Furthermore, they make strong assumptions such as: a corrupt device voluntarily tries to correct itself; every device in the network can perform securely route messages to other honest devices despite the presence of a Byzantine adversary in the network.

Regarding code updation, N. Asokan et al. extended The Update Framework [34] and proposed an architecture for secure firmware update [9]. This work takes various stakeholders such as manufacturer, software distributor, domain controller and end devices in IoT firmware update ecosystem; and establishes an end-to-end security between devices manufactures and IoT devices. This work also suffers from the limitations described in §5.

10 CONCLUSION

In this paper, we presented AIRMED - a novel decentralized, scalable, efficient, and secure mechanism of recovering a network of heterogeneous low-end devices in the presence of self-propagating malware. Furthermore, unlike prior works, AIRMED guarantees update of entire network. For efficiency, we used bloom-filters to identify compromised code chunks, random back-off and stream signatures to reduce bandwidth overhead and enhance security. Evaluation, of our approach using OMNeT++, illustrates that AIRMED scales upto 1000s of device and can recover the entire network in minutes. We also evaluated the memory and communication costs of AIRMED and showed that it incurs very low overhead. Addressing these issues with dynamic swarms and run-time attacks could be an interesting avenue for future researches.

ACKNOWLEDGMENTS

The authors would like to thank Nitin Awathare, Aashish Kolluri, Jong Chan Lee, Archit Patke, Soundarya Ramesh, Ling Ren, and Qi Wang for helpful discussion and feedback on the early version of the paper.

REFERENCES

- [1] 2018. TrustLite, A Platform Security Framework for Tiny Embedded Devices. (2018). https://www.informatik.tu-darmstadt.de/systemsecurity/research/sys/projects/previous_projects/trust_lite/nd_embedded_systems/trustlite/trustlite_1_en.jsp
- [2] 2019. Gartner Says a Thirty-Fold Increase in Internet-Connected Physical Devices by 2020 Will Significantly Alter How the Supply Chain Operates. (2019). <http://www.gartner.com/newsroom/id/2688717>
- [3] 2020. Gods and Goddesses of Healing. (2020). <https://www.learnreligions.com/gods-and-goddesses-of-healing-2561980>
- [4] 2020. OpenSim Ltd. OMNeT++ discrete event simulator. (2020). <http://omnetpp.org/>.
- [5] Moreno Ambrosin, Mauro Conti, Ahmad Ibrahim, Gregory Neven, Ahmad-Reza Sadeghi, and Matthias Schunter. 2016. SANA: secure and scalable aggregate network attestation. In *Proceedings of the 2016 ACM SIGSAC Conference on Computer and Communications Security*. ACM, 731–742.
- [6] Moreno Ambrosin, Mauro Conti, Riccardo Lazzaretto, Md Masoom Rabbani, and Silvio Ranise. 2018. PADS: Practical Attestation for Highly Dynamic Swarm Topologies. *arXiv preprint arXiv:1806.05766* (2018).

- [7] Manos Antonakakis, Tim April, Michael Bailey, Matt Bernhard, Elie Bursztein, Jaime Cochran, Zakir Durumeric, J Alex Halderman, Luca Invernizzi, Michalis Kallitsis, et al. 2017. Understanding the mirai botnet. In *26th {USENIX} Security Symposium ({USENIX} Security 17)*. 1093–1110.
- [8] N Asokan, Ferdinand Brasser, Ahmad Ibrahim, Ahmad-Reza Sadeghi, Matthias Schunter, Gene Tsudik, and Christian Wachsmann. 2015. Seda: Scalable embedded device attestation. In *Proceedings of the 22nd ACM SIGSAC Conference on Computer and Communications Security*. ACM, 964–975.
- [9] N Asokan, Thomas Nyman, Norrathep Rattanavipanon, Ahmad-Reza Sadeghi, and Gene Tsudik. 2018. ASSURED: Architecture for Secure Software Update of Realistic Embedded Devices. *IEEE Transactions on Computer-Aided Design of Integrated Circuits and Systems* 37, 11 (2018), 2290–2300.
- [10] Amin Azmoodeh, Ali Dehghantanha, and Kim-Kwang Raymond Choo. 2018. Robust malware detection for internet of (battlefield) things devices using deep eigenspace learning. *IEEE Transactions on Sustainable Computing* (2018).
- [11] Elisa Bertino and Nayeem Islam. 2017. Botnets and internet of things security. *Computer* 2 (2017), 76–79.
- [12] Karthikeyan Bhargavan, Bruno Blanchet, and Nadim Kobeissi. 2017. Verified models and reference implementations for the TLS 1.3 standard candidate. In *2017 IEEE Symposium on Security and Privacy (SP)*. IEEE, 483–502.
- [13] Ferdinand Brasser, Brahim El Mahjoub, Ahmad-Reza Sadeghi, Christian Wachsmann, and Patrick Koeberl. 2015. TyTAN: tiny trust anchor for tiny devices. In *Proceedings of the 52nd Annual Design Automation Conference*. ACM, 34.
- [14] Xavier Carpent, Karim ElDefrawy, Norrathep Rattanavipanon, and Gene Tsudik. Lightweight swarm attestation: a tale of two LISA-s. In *Proceedings of the 2017 ACM on Asia Conference on Computer and Communications Security*.
- [15] Dung Dang, Mione Plant, and Mehrvash Poole. 2018. Wireless connectivity for the Internet of Things (IoT) with MSP430™ microcontrollers (MCUs). (2018). <https://www.ti.com/lit/wp/slay028/slay028.pdf>
- [16] Kaustubh Dhondge, Rajeev Shorey, and Jeffrey Tew. 2016. Hola: Heuristic and opportunistic link selection algorithm for energy efficiency in industrial internet of things (iiot) systems. In *2016 8th international conference on communication systems and networks (COMSNETS)*. IEEE, 1–6.
- [17] Karim Eldefrawy, Gene Tsudik, Aurélien Francillon, and Daniele Perito. 2012. SMART: Secure and Minimal Architecture for (Establishing Dynamic) Root of Trust.. In *NDSS*, Vol. 12. 1–15.
- [18] Earlene Fernandes, Jaeyeon Jung, and Atul Prakash. 2016. Security analysis of emerging smart home applications. In *2016 IEEE Symposium on Security and Privacy (SP)*. IEEE, 636–654.
- [19] Rosario Gennaro and Pankaj Rohatgi. 1997. How to sign digital streams. In *Annual International Cryptology Conference*. Springer, 180–197.
- [20] Hamed Haddadpajouh, Ali Dehghantanha, Raouf Khayami, and Kim-Kwang Raymond Choo. 2018. A deep Recurrent Neural Network based approach for Internet of Things malware threat hunting. *Future Generation Computer Systems* (2018).
- [21] Yih-Chun Hu, Adrian Perrig, and David B Johnson. 2005. Ariadne: A secure on-demand routing protocol for ad hoc networks. *Wireless networks* (2005).
- [22] Ahmad Ibrahim, Ahmad-Reza Sadeghi, and Gene Tsudik. 2018. AID: autonomous attestation of IoT devices. In *SRDS*.
- [23] Ahmad Ibrahim, Ahmad-Reza Sadeghi, and Gene Tsudik. 2019. Healed: Healing & attestation for low-end embedded devices. In *International Conference on Financial Cryptography and Data Security*. Springer, 627–645.
- [24] Brian Jalaian, Timothy Gregory, Niranjani Suri, Stephen Russell, Laurel Sadler, and Michael Lee. Evaluating LoRaWAN-based IoT devices for the tactical military environment. In *2018 IEEE 4th World Forum on Internet of Things (WF-IoT)*.
- [25] Frank T Johnsen, Zbigniew Zieliński, Konrad Wrona, Niranjani Suri, Christoph Fuchs, Manas Pradhan, Janusz Furtak, Bogdan Vasilache, Vincenzo Pellegrini, Michał Dyk, et al. Application of IoT in military operations in a smart city. In *2018 International Conference on Military Communications and Information Systems (ICMCIS)*. IEEE.
- [26] Adam Kirsch and Michael Mitzenmacher. 2006. Less hashing, same performance: building a better bloom filter. In *European Symposium on Algorithms*. Springer.
- [27] Patrick Koeberl, Steffen Schulz, Ahmad-Reza Sadeghi, and Vijay Varadharajan. 2014. TrustLite: A security architecture for tiny embedded devices. In *Proceedings of the Ninth European Conference on Computer Systems*. ACM, 10.
- [28] Florian Kohnhäuser and Stefan Katzenbeisser. 2016. Secure code updates for mesh networked commodity low-end embedded devices. In *European Symposium on Research in Computer Security*. Springer, 320–338.
- [29] Constantinos Kolias, Georgios Kambourakis, Angelos Stavrou, and Jeffrey Voas. 2017. DDoS in the IoT: Mirai and other botnets. *Computer* 50, 7 (2017), 80–84.
- [30] Deepak Kumar, Kelly Shen, Benton Case, Deepali Garg, Galina Alperovich, Dmitry Kuznetsov, Rajarshi Gupta, and Zakir Durumeric. 2019. All things considered: an analysis of IoT devices on home networks. In *28th {USENIX} Security Symposium ({USENIX} Security 19)*. 1169–1185.
- [31] Di Ma, Claudio Soriente, and Gene Tsudik. 2009. New adversary and new threats: security in unattended sensor networks. *IEEE network* 23, 2 (2009), 43–48.
- [32] Michael Mitzenmacher and Eli Upfal. 2017. *Probability and computing: randomization and probabilistic techniques in algorithms and data analysis*. Cambridge

- university press.
- [33] Eyal Ronen, Adi Shamir, Achi-Or Weingarten, and Colin O'Flynn. 2017. IoT goes nuclear: Creating a ZigBee chain reaction. In *2017 IEEE Symposium on Security and Privacy (SP)*. IEEE, 195–212.
- [34] Justin Samuel, Nick Mathewson, Justin Cappos, and Roger Dingledine. 2010. Survivable key compromise in software update systems. In *Proceedings of the 17th ACM conference on Computer and communications security*. ACM, 61–72.
- [35] Arvind Seshadri, Mark Luk, Adrian Perrig, Leendert van Doorn, and Pradeep Khosla. 2006. SCUBA: Secure code update by attestation in sensor networks. In *Proceedings of the 5th ACM workshop on Wireless security*. ACM, 85–94.
- [36] Arvind Seshadri, Adrian Perrig, Leendert Van Doorn, and Pradeep Khosla. 2004. Swatt: Software-based attestation for embedded devices. In *null*. IEEE, 272.
- [37] Saleh Soltan, Prateek Mittal, and H Vincent Poor. 2018. BlackIoT: IoT Botnet of high wattage devices can disrupt the power grid. In *27th {USENIX} Security Symposium ({USENIX} Security 18)*. 15–32.
- [38] George Spanogiannopoulos, Natalija Vljajic, and Dusan Stevanovic. 2009. A simulation-based performance analysis of various multipath routing techniques in ZigBee sensor networks. In *International Conference on Ad Hoc Networks*. Springer, 300–315.
- [39] Lawrence J Trautman and Peter C Ormerod. 2017. Industrial cyber vulnerabilities: Lessons from Stuxnet and the Internet of Things. *U. Miami L. Rev* (2017), 761.
- [40] Deepak Vasisht, Zerina Kapetanovic, Jongho Won, Xinxin Jin, Ranveer Chandra, Sudipta Sinha, Ashish Kapoor, Madhusudhan Sudarshan, and Sean Stratman. 2017. Farmbeats: An iot platform for data-driven agriculture. In *14th {USENIX} Symposium on Networked Systems Design and Implementation ({NSDI})*.
- [41] Alessandro Visintin, Flavio Toffalini, Mauro Conti, and Jianying Zhou. 2019. SAFE^d: Self-Attestation For Networks of Heterogeneous Embedded Devices. *arXiv preprint arXiv:1909.08168* (2019).
- [42] Yang Wang, Deepayan Chakrabarti, Chenxi Wang, and Christos Faloutsos. Epidemic spreading in real networks: An eigenvalue viewpoint. In *22nd International Symposium on Reliable Distributed Systems, 2003. Proceedings*. IEEE.
- [43] Samuel Wedaj, Kolin Paul, and Vinay J Ribeiro. 2019. DADS: Decentralized attestation for device swarms. *ACM Transactions on Privacy and Security (TOPS)* (2019).
- [44] Seung Yi, Prasad Naldurg, and Robin Kravets. 2001. Security-aware ad hoc routing for wireless networks. In *Proceedings of the 2nd ACM international symposium on Mobile ad hoc networking & computing*. ACM, 299–302.
- [45] Cliff Changchun Zou, Weibo Gong, and Don Towsley. 2002. Code red worm propagation modeling and analysis. In *Proceedings of the 9th ACM conference on Computer and communications security*. ACM, 138–147.

A ALGORITHMS

Algorithm 1 selfcheck

```

1: Input  $ak_i, v_i, [\text{code}]$ 
2:  $v'_i \leftarrow \text{attest}(ak_i, [\text{code}])$ 
3: if  $v'_i = v_i$  then
4:    $\lambda \leftarrow \max\{\lambda/(\lambda + 1), \lambda_{\min}\}; \delta \leftarrow \exp\{\lambda\}$ 
5:   enable interrupt; resume application.
6: else
7:   mark [code] as non-executable.
8:   rectify()

```

Algorithm 2 handleCodeRequest at device $n_j \in N_i$

```

1: input  $\text{MSG}_{\text{req}} = \langle \text{ttl}, s_i, |N_i|, z_i, b, \Pi \rangle$ 
2: global  $A_j, \Delta, \theta, \lambda, \lambda_{\max}$ 
3: if  $b \in A_j$  then
4:    $z_j \leftarrow \text{ver}(b)$ 
5:   if  $z_j \geq z_i$  then
6:      $\tau_j \leftarrow (\Delta - (z_j - z_i))|N_i|\theta + \lceil \mathcal{U}(0, 1)|N_i| \rceil \theta$ 
7:     set transmit code timer after  $\tau_j$ 
8: if  $\text{ttl} > 0$  then
9:    $\lambda \leftarrow \min\{2\lambda, \lambda_{\max}\}; \text{ttl} \leftarrow \text{ttl} - 1$ 
10: if  $\text{ttl} > 0$  then
11:   broadcast a message warning devices in  $N_j$ 

```

Algorithm 3 handleCodeResponse at device n_i

```

1: input  $\Pi$ 
2: while true do
3:   new response  $\text{MSG}_{\text{resp}} = \langle \{\text{pos}_j, \text{data}_j\} \rangle$ 
4:   while next  $\text{pos} \in \{\Pi \cap \text{MSG}_{\text{resp}}\}$  do
5:      $\text{data} \leftarrow \text{MSG}_{\text{resp}}[\text{pos}]$ 
6:     if stream signature of data is valid then
7:       load data to code;
8:        $\Pi \leftarrow \Pi \setminus \text{pos}; \text{MSG}_{\text{resp}} \leftarrow \text{MSG}_{\text{resp}} \setminus \{\text{pos}, \text{data}\}$ 
9:     else
10:      break
11:   if  $\Pi$  is empty then
12:      $\lambda \leftarrow \lambda_{\max}$ ; update interrupt handler
13:     broadcast  $\text{MSG}_{\text{done}}$ ; restart  $n_i$ 
14:   else
15:      $\delta \leftarrow \exp\{\lambda\}$ 
16:     re-broadcast  $\text{MSG}_{\text{req}}$  after  $\delta$  time interval.

```

B NOTATION TABLE

Notation	Description
\mathcal{O}	Network operator/Owner
$pk_{\mathcal{O}}, sk_{\mathcal{O}}$	public-private key pair of \mathcal{O}
N	Total number of nodes in the network
n_i	i^{th} device
pk_i, sk_i	public-private key pair of n_i
B_i, C_i	Application binaries executed and stored by n_i
N_i	Neighbors of n_i after successful rendezvous
$N_i^{(b)}$	Devices in N_i that runs/stores binary b
k_i	Symmetric key shared by n_i
q_i	Sequence number of n_i
λ	Self-check rate
ak_i, v_i	Attestation key and value at n_i
$F, L = \{l_j\}$	Bloom filter and the corresponding keys
$\mathcal{A}_{\text{int}}, \mathcal{A}_{\text{ext}}$	Internal and External Adversary resp.
$\lambda_{\text{int}}, \lambda_{\text{ext}}$	Corruption rate of \mathcal{A}_{int} , and \mathcal{A}_{ext}

C PROOFS

To prove Theorem 6.2 we will first prove Lemma C.1. Let the time interval where devices running an identical version of the code, transmits the requested chunk be called as an *epoch*. Observe that, each epoch $m\theta$ long. Let each epoch be divided into m time intervals called a *slot*. Note that, in AIRMED devices running different versions always sends the requested chunks in disjoint epochs. Also, within an epoch, once an honest device sends the requested chunk, the recipient device broadcasts to each of its neighbors to stop them from redundantly sending the same chunks (ref. §4.2). Hence, if only neighbor sends the requested chunk in the first non-empty slot, there would be no-redundancy at all.

LEMMA C.1. *Let there be m neighbors running the same version of application b for any given device. Also, let X^j for $1 \leq j \leq m - 1$ be the random variable denoting the number of devices which sends the requested chunks in slot j when the remaining $m - X^j$ nodes transmits*

in a slot greater than j . Then,

$$\Pr[X^j = k] = \frac{\binom{m}{k}(m-j)^{(m-k)}}{m^m} \quad (7)$$

PROOF. We use counting arguments to prove this theorem. There are total m^m possibilities of arranging m devices in m slot. Among these possibilities, the number of ways $X_j = k$ can occur if: (i) Any subset of k devices transmits in slot j ; there are $\binom{m}{k}$ possible ways of selecting these devices. and (ii) the remaining $m - k$ device transmits in slots $j + 1$ to m ; there are $(m - j)^{m-k}$ ways of doing this. Putting them together gives us the desired result. \square

COROLLARY C.2. *The probability that only one neighbor device will transmit the requested code in the situation described above is:*

$$\Pr[\text{One device transmits code}] = \sum_{j=1}^{m-1} \left(1 - \frac{j}{m}\right)^{(m-1)} \quad (8)$$

PROOF. (Theorem 6.2) The first term directly follows Lemma C.1 and the second term corresponds to the case where all device transmits the requested chunk in the m^{th} slot. \square

PROOF. (Theorem 6.4) Let \mathbf{H}_b denote the set of honest devices at any given time after t_0 , by our assumption $|\mathbf{H}_b| > 0$. Consider a corrupt or blank device $n_d \in G_b$ which is initially v hops away from the nearest honest device in $n_h \in \mathbf{H}_b$ and n_a be the penultimate node on the path from n_d to n_h . By definition, n_a is corrupt. After an exponentially distributed waiting time, n_a performs a self-check and recovers itself one of its honest neighbors. This is guaranteed to happen since $n_h \in N^{(b)}_a$. Thus d_i now joins \mathbf{H}_b . This reduces the distance between n_d and the nearest honest by at least one unit. Since, there are only finite number of nodes in the network, this distance will eventually become zero. \square

PROOF. (Theorem 6.5) Let $U_b \subseteq G_b$ be the set of updated devices at time t_0 . By definition all non-updated devices in the neighbourhood of devices in U_b . Thus, whenever one of these devices say n_v performs self-check, it will get updated with the newer version and join U_b . Device n_v then broadcast the newer version to update all non-updated honest devices in its neighborhood. Hence, the number of updated device increases by at least one. Since, there are only finite number of devices, eventually the entire network will get updated. \square